Atlas Journal of Materials Science 2 (2): 65–72, 2015
doi: 10.5147/ajms.2015.0167

Challenges to Fabricate Large Size-Controllable Submicron-Structured Anodic-Aluminum-Oxide Film

Jin Shyong Lin[1], Shih Hsun Chen[2], Ker Jer Huang[3], Chien Wan Hun[4*], and Chien Chon Chen[5*]

[1] Department of Mechanical Engineering, National Chin-Yi University of Technology, Taichung 41170, Taiwan; [2] Department of Engineering Technology and Industrial Distribution, Texas A&M University, College Station, Texas 77845, USA; [3] Chung-Shan Institute of Science and Technology, Taoyuan 32546, Taiwan; [4] Department of Mechanical Engineering, National United University, Miaoli 30063, Taiwan; [5] Department of Energy Engineering, National United University, Miaoli 30063, Taiwan.

Received: November 13, 2015 / Accepted: November 24, 2015

Abstract

Anodic aluminum oxide (AAO) is well known for its unique controllable structure and functional contributions in research and developments. However, before AAO can be widely used in the industry, some engineering problems should be overcome. In this study, we designed a novel electrochemical mold, which can resolve the exothermal problem for large-size aluminum sheets during high-voltage anodization process. AAO film with a large sample size of 11 x 11 cm^2 in area, 148 μm in thickness and 450 nm in average pore diameter, decorated with ordered-pattern structure, was successfully obtained through a 200 V anodization process. It was noticed that the local heat was generated with increasing the anodizing voltage, resulting in undesired pits and burr defects on the AAO surface. In order to retain AAO's quality and reduce the producing cost of the anodization process, a mass producing system combining with an overhead conveyor was proposed. The convenient anodization system, novel electrochemical mold and bath may help to fabricate high-quality AAO films efficiently.

Keywords: Anodic aluminum oxide (AAO); Electrochemistry; Large pore size; Exothermal reaction; Mass production.

Introduction

Anodization is an electrochemical treatment to form a dense oxide film on the surface. Anodic treatment is conventionally applied for surface corrosion resistance, painting, electrical insulation, electroplating, and wear resistance. The anodic oxide film made by anodic treatment usually possesses a porous structure; therefore, a post sealing process must be applied to the anodic oxide film to facilitate the formation of dense anodic oxide membrane. Anodizing treatment has the advantages of low cost, rapid production and the capability to obtain large-scaled products, such as dye-sensitized solar cells, thermal conductive sheets, super capacitors and thermal insulating components (Chen et al., 2013; Chen et al., 2013; Chen et al., 2013; Chen et al., 2011). To date, many producing system have been developed to achieve anodized aluminum oxide (AAO) coating, including sulfuric acid, oxalic acid, phosphoric acid, or their mixture thereof as an electrolyte, with a suitable DC voltage supplier.

At present the structure-controllable AAO films have been widely studied in the academia. AAO can be directly applied to nanometer or submicron processes, and the templates with nanometer or submicron pores of aluminum oxide have the potentials for various product applications (Chen et al., 2004; Chen et al., 2013; Chen et al., 2013; Chen et al., 2009). However, due to the lack of scale-up facilities, AAO has not yet been commonly-

* Corresponding authors: monger@nuu.edu.tw (Chien Wan Hun); chentexas@gmail.com (Chien Chon Chen).

utilized in industries and research organizations, such as semiconductor industry, optoelectronic industry, biomedical industry, universities and laboratories. In the past years, many excellence characterizations of AAO have been published in the academic research, but it was still difficult to find out AAO-related products on the market. In order to bring AAO from the academic laboratory to the industry, in this study some key issues will be addressed and their solutions are proposed.

AAO template has the structure of a large surface area, good mechanical strength and flexibility, which is thought to be a good candidate material for the nano- and submicron membranes. It is believed that AAO has a lower melting point than pure alumina because of the inclusions in the porous AAO structure. Spooner (Spooner, 1955) presented that the alumina film anodized in a sulfuric acid solution was composed of Al2O3 (78.9%), Al_2O_3.H_2O (0.5%), $Al_2(SO_4)_3$ (20.2%), and H_2O (0.4%). According to Lee's study (Lee et al., 2008), the melting point of AAO is close to 1200 °C. Moreover, AAO template was stable below 1000 °C (Mardilovich et al., 1995), which was much lower than that of bulk alumina (2017 °C for $Al_2O_3(\gamma)$) (Barin, 1989). However, the stabilizing temperature for AAO structure is high enough for serving as a template for most polymers, ceramics or alloys.

In order to obtain a high-quality AAO template, many procedures should be carried out sequentially with the aluminum sheet (Chen et al., 2012). For example, the fabrication processes for 10 nm AAO template consist of the following steps:

(1) Annealing: a high-purity Al (5 N) sheet was annealed in an air furnace at 550 °C for 1h.
(2) Mechanical grinding and polishing: the annealed Al sheet was grinded with #2000-grit sand paper and then polished with 0.3 μm Al_2O_3 powder slurry.
(3) Electrolytic polishing: the polished Al sheet was further electro-polished in the electrolyte composed of 15 vol.% $HClO_4$ +70 vol.% C_2H_6O + 15 vol.% $CH_3(CH_2)_3OCH_2CH_2OH$ solution at 42 V and 25 °C for 10 min.
(4) The first anodization: the electropolished Al sheet was anodized in 5 wt.% H_2SO_4 solution at 10 V and 5 °C for 30 min.
(5) AAO removing: the first AAO film was removed by immersing in the solution of 1.8 wt.% CrO_3 + 6 vol.% H_3PO_4 solution at 70 °C for 30 min.
(6) The second anodization: the Al sheet was anodized for the 2nd time in the same electrolyte as step (4) for 1 h.
(7) Al substrate removing: the remaining Al sheet was removed in the solution of 10 wt.% $CuCl_2$ + 8 vol.% HCl solution at 25 °C for 5 min.
(8) Barrier layer removing: the bottom of AAO film was removed in 5 vol.% H_3PO_4 solution at 20 °C for 30 min.
(9) Pore widening: the channel structure of AAO film was modified in 5 vol.% H_3PO_4 solution at 20 °C for 1 min.

Based on the above steps when the voltage and electrolyte (steps 4 and 6) are change to 40 V and 3 wt.% $C_2H_2O_4$, the AAO with the pore size of 40 nm can be formed. When the 40 nm AAO was immersed in the H_3PO_4 solution (step 9) the AAO's pore size can be expended to 90 nm maximally. When the voltage and electrolyte (steps 4 and 6) are change to 180 V and 1 vol.% H_3PO_4, the 160 nm AAO can be synthesized. While when the 160 nm AAO was immersed in the H_3PO_4 solution (step 9) the AAO pore size can be expend to 400 nm maximally. According to the AAO fabrication processes in various acid systems, the AAO with pore sizes between 10 to 400 nm AAO can be obtained.

Since the AAO processes are sensitive to the operation conditions, defects would appear in AAO templates if unsuitable conditions are applied. The controllable conditions include temperature, applied voltage, electrolyte composition, cooling stirring, and current density distribution. In the anodization process, the working electrode presents an exothermic reaction. Thus, when preparing small-scale samples for academic research, it is not a problem to deal with small quantity of heat from the exothermic reaction. In mass production process, however, maintenance of constant current density and temperature become critical issues. In this study, we designed the electrochemical mold, the chemical bath, and the AAO mass production system. The useful tools helped to successfully produce large-size submicron-structured tubular films. High-quality and inexpensive AAO is a potential material for both academic research and industrial applications.

Experimental Procedures

The experimental raw metal for anodization was a high-purity aluminum plate (Al, 99.999%). AAO film was obtained through a series of mechanical working, electrochemical reaction and chemical reaction processes, including annealing, mechanical grinding and polishing, electrolytic polishing, the first anodization, AAO removing, the second anodization, barrier layer removing, and pore widening steps. The submicron-structured AAO was synthesized at 200 V in 1 vol.% H_3PO_4 electrolyte at 1 °C conditions, and its growing rate was about 5 μm/h in thickness. The remaining Al substrate was removed by immersed in 10 wt.% cupric chloride + 8 vol.% hydrochloric acid (HCl) solution, and then cleaned thoroughly in distilled water. The obtained samples were mainly characterized by a scanning electron microscope (SEM, JEOL JSM-7500) and optical microscope (Nikon LV 150). For the SEM observation, a thin Pt or Pd/Pt layer (~3 nm) was deposited on the sample surface to form a conductive film to avoid charging effect.

For a large-size AAO fabrication, the electrolytic polished Al sheet was set in the electrochemical mold for anodization. Silicone rubber chips were used for the waterproof, and the anodic voltages were applied onto the Al plates through an electrode rod, contacting with a supporting electrode plate. A stirrer motor was used to remove exothermal heat generated from anodic Al surface. The anodic area was defined by the mold's open area.

Results and Discussion

Electrochemical techniques can be used in the various field, such as deposition, anodization, etching, polishing, pitting, and corrosion applications. A basic electrochemical reaction system is composed of an anode, a cathode, and the electrolyte; additionally, they can provide different functions in various electrochemical reactions. For example, the anode acts as a working

electrode and the cathode is a counter one during anodizing, etching, pitting, and corrosion reactions. However, the anode can also be a counter and the cathode can be a working electrode during electrodeposition.

Figure 1 shows the schematic diagrams of four basic electrochemical applications. (a) Electrodeposition: the positive-charged ions (M^+) deposited on the working electrode (cathode). The charged ions move from the anode to cathode surface through electrolyte, and the electrons move in the same direction through inner connection circuit to the surface of cathode. Finally, the positive-charged ions combine with the electrons to form precipitate onto the working electrode. (b) Anodization: the negative-charged ions (OH^-) move through electrolyte to the anode surface and react with positive-charged ions (M^+) to form an oxide layer on the working electrode (anode). The electrons move from the anode to the cathode through inner connection circuit. Finally, the positive charge reacts with the negative-charged ions to form an anodic film on the working electrode. (c) Etching: the positive-charged ions (M+) are dissolved from the anode and dispersed into the electrolyte, and the electrons move from the anode to the cathode through inner connection circuit. Finally, pits or rough surface form on the working electrode (anode). (d) Electropolishing: the mechanism is the same as (c) but for different electrolyte and conditions. Finally, the smooth surface present on the working electrode (anode).

The high-quality anodic film can be controlled through electrochemical parameters, including electrolyte temperature, electrolyte composition, electrolyte flow distribution, anodic voltage, current density, the distance between anode and cathode, the anode area relative to the cathode area, and the bobbles effect on the electrodes. In order to have an accurate control of electrochemical conditions, the power supply, reaction bath, and electrochemical mold are designed for the demands for anodization process specifically. The structure-controllable AAO is a well-known technology in the research for academic purposes. However, for wide applications in industry, some engineering problems should be overcome in advance; especially for the purposes to obtain AAO with large-size areas, thick film, submicron porous structure, and high film formation rate. Here, we propose an electrochemical mold design which assists high-quality and a large-size AAO fabrication.

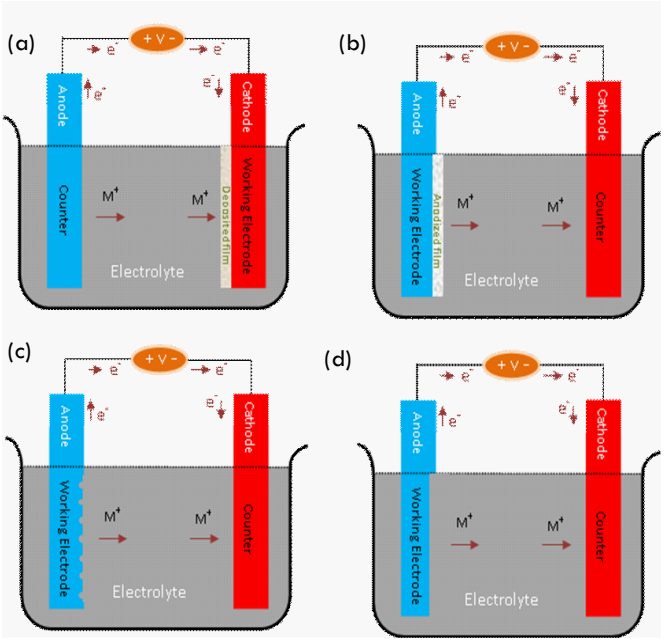

Figure 1. Schematic of electrochemical reaction; (a) deposition, (b) anodization, (c) etching, (d) polishing.

The endothermal or exothermal effects always occur along with the electrochemical reactions. Especially, for a large-scale electrochemical reaction the thermal effects are obvious. This thermal effect may rise the electrolyte temperature into an unstable state. A good electrochemical mold can reduce the thermal effects and stabilize the workpiece's temperature.

The anodic voltage determines the pore size of AAO film. Two experience formulas are commonly used to estimate the pore size and the pore distance of AAO. The pore size varied with voltage is C = mV, where C is cell size (nm), V is anodizing voltage (V), and m is a constant (2-2.5). The pore distance varied with voltages is V = (2R-10)/2, where 2R is spacing distance (5-1000 nm) (Ying et al., 1998). Because of the anodic exothermal effect, to produce a thick AAO film with submicron pore is a challenging task; for example, to fabricate 400-500 nm pore size under a 200 V anodization voltage.

During the higher voltage anodization, pits are easily generated on the AAO surface, resulting in a failure of AAO film. As shown in Figure 2, the burring point prefers to present at the sample corner during anodization. Fig. 2(a) shows a fixed Al anodic surface by the assistance of silicone rubber; Fig. 2(b), a starring bobble formation at the interface of silicone rubber chip-anodic surface; Fig. 2(c), local pitting continues forming at the interface; sequentially; and Fig. 2(d), burring zone expands from the interface and then to the bulk Al.

Figure 3 shows the real image of AAO burring during anodization, including a starring pitting forming at the interface of silicone rubber chip-anodic surface (Fig. 3a), a starring burning zone (Fig. 3b), burning zones on Al border (Fig. 3c), and a larger area of burring zone on the AAO after a long-time anodization (Fig. 3d).

Figure 4 further shows the images of pitting and burring zone forming on the Al surface during anodization. In Figure 4 (a), a high-purity aluminum substrate presents the microstructure of large grains with small pits in the beginning of anodization. A large pit is formed on the Al surface under 200V anodization for 1 min, as shown in Figure 4 (b). Local and entire burring zone formed on the AAO under 200 V anodization after 10 and 30 min, as shown in Figures 4(c) and (d), respectively.

Because the heat generation always occurs when metals or components are ionized, the AAO electrolyte must be kept at a low or room temperature during entire processes. In AAO processes, the ionization reactions may include Eqns. 1 to 5, which are all exothermic reactions (Chen et al., 2005), where ΔH_f^0 is standard enthalpy.

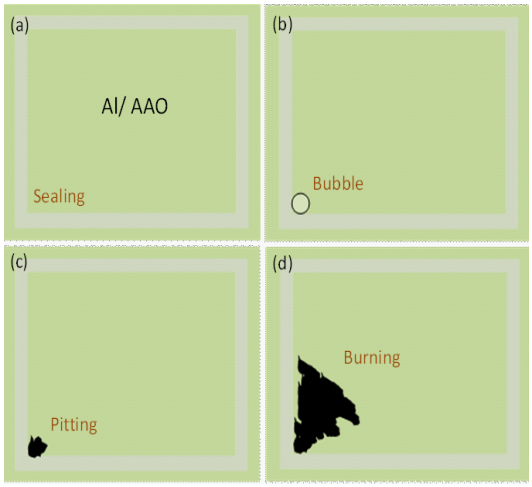

Figure 2. Schematic diagram of AAO burring during anodization; (a) before anodization, (b) bobble formation on corner, (c) local pitting formation, (d) burring zone formation.

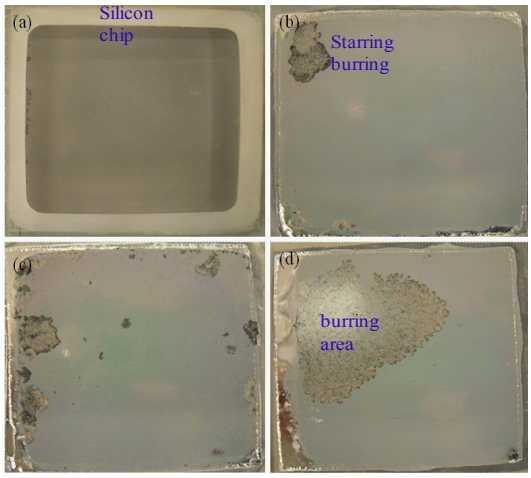

Figure 3. Optical images of AAO burring during anodization; (a) before anodization, (b) a starring burning zone, (c) burning zones, (d) a larger area of burring zone.

$$H_2SO_4 \rightarrow 2H^+ + SO_4^{2-};\ \Delta H_f^o = -909.3\ \text{kJ} \quad (1)$$

$$H_3PO_4 \rightarrow 3H^+ + PO_4^{3-};\ \Delta H_f^o = -1277.4\ \text{kJ} \quad (2)$$

$$C_2H_2O_4 \rightarrow 2H^+ + C_2O_4^{2-};\ \Delta H_f^o = -818.3\ \text{kJ} \quad (3)$$

$$Al \rightarrow Al^{3+};\ \Delta H_f^o = -531.4\ \text{kJ} \quad (4)$$

$$H_2O \rightarrow H^+ + OH^-;\ \Delta H_f^o = -230.1\ \text{kJ} \quad (5)$$

Eqns. 1-3 mean that the acids dissolve in the electrolytes as the exothermic reactions. The quantity of dissolving heat is directly proportional to the acid concentration. Eqn. 4 shows the exothermic heat generated from Al ionization. The quantity of ionization heat is directly proportional to the anodizing voltage.

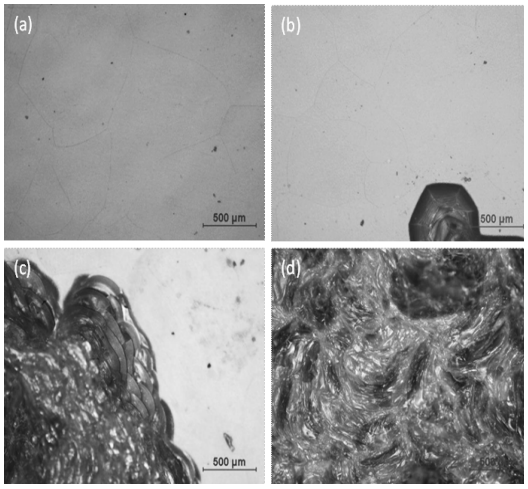

Figure 4. Optical micro-images of pitting and burring zone formation on the Al surface during anodization; (a) high purity aluminum substrate with large grains, (b) pitting formation on the Al surface during anodization, (c) local burring zone formation on the Al surface, (d) large burring area on the Al surface.

The exothermic heat of Eqns. 1 to 3 could be eliminated before anodization by cooling down the solution in an isothermal bath. However, the exothermic reactions of Eqns. 4 and 5 happen during anodizing, the so-called local heat. The local heat should be quickly removed by cycling or agitating the electrolyte; otherwise, local pits, burring, or cracking would form on AAO surface.

Applied anodic voltages define the working conditions of sample falling at an anodizing or pitting region, which increases with the voltage stepping-up rate. The higher voltage is applied, the severer electrochemical reactions occur. Therefore, the oxide film will initially break down due to the mechanical stress caused by gas evolving from the AAO. Then, aggressive ions of $C_2O_4^{-2}$, SO_4^{-2}, or PO_4^{-3} are adsorbed at the bare metal and enhance active dissolutions. The grain boundaries of Al substrate always reduce the ordering of nanopores on AAO. High concentration of attacking ions (such as SO_4^{-2}, $C_2O_4^{-2}$, and PO_4^{-3}) causes the selective etching at grain boundaries more easily. Moreover, an unstable current density caused sub-branched nanopores to appear. The above issues may not affect the quality of a small AAO sample, but those fabrication parameters will decide the final quality of AAO film when fabricate a large amount or area of AAO products at the same time.

Figure 5 shows the images of pitting forming on the Al surface during anodization. In Figure 5 (a), the high-purity aluminum is presented with large grains. Figure 5 (b) further shows the initial pits forming at the grain boundaries anodized at 100 V for 10 sec. When the applied increased to 150 V, more local pits formed on the Al grain for 10 sec, as shown in Figure 5 (c). In Figure 5 (d), a large pit formed on Al substrate with an anodizing voltage of 200 V for 10 sec. When a lower anodic voltage was applied on Al surface, the initial pits formed on the grain boundaries. However; many pits would directly form on the grains while a higher anodic voltage was applied. For example, Figure 6 shows the small local AAO burning and pits on the Al surface under a higher anodic voltage. Pits are of a high aspect

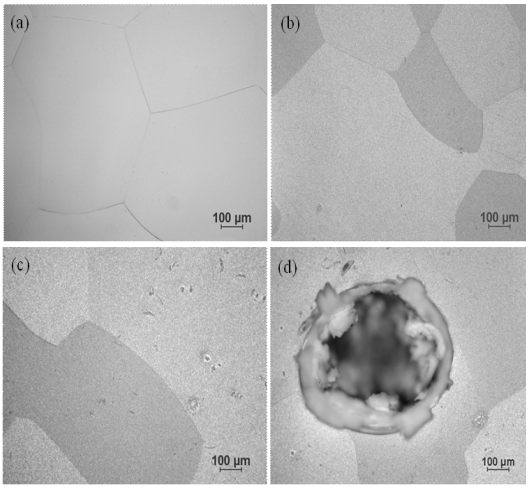

Figure 5. Optical micro-images of Al surface with electro-polishing and anodization treatment. (a) high purity aluminum surface after electro-polishing, (b) aluminum surface after 100 V for 10 sec anodization, (c) aluminum surface after 150 V for 10 sec anodization, (d) aluminum surface after 200 V for 10 sec anodization.

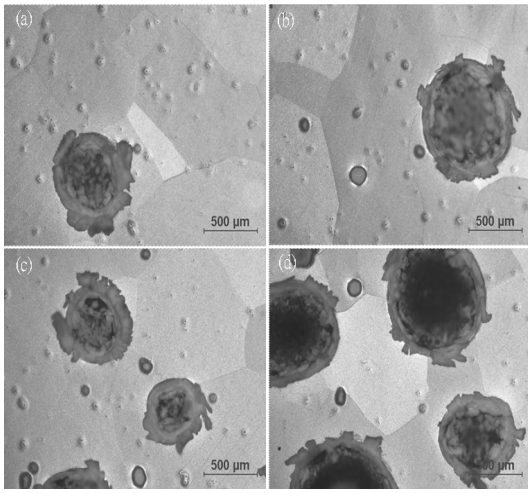

Figure 6. Optical micro-images of pitting formation on AAO under a higher anodic voltage applied; (a) the initial pits formation on the Al grains, (b) pit growth, (c) pits growth, (d) many pits growth on the AAO surface after lasting anodization.

ratio, and their large surface areas promoted severe chemical reactions, causing the fresh anodic film continue burring. Figure 6 (a) shows the initial small pits dispersed in the Al grains, with a large pit formed there. A series of pit's growth on the AAO surface after lasting anodization are recorded in Figures 6 (b)-(d).

The reactions of water dissolving (reaction 6) and aluminum oxide formation (reaction 7 and 8) may occur on the Al surface during anodization. Based on the reactions (6) and (7), the O2 and H2 gases form on Al surface, which may retain or cover the surface during insufficient circulation or agitation of electrolyte. A local heat, especially on the mold edges, would therefore burn the anodic oxide film to form the pitting. Furthermore, the number of pits increases to form a large burring area as the anodization lasts.

$$2H_2O \rightarrow O_2 + 4H^+ + 4e^- \quad (6)$$

$$2Al^{3+} + 3OH^- \rightarrow Al_2O_3 + 1.5H_2 \quad (7)$$

$$2Al^{3+} + 3O^{2-} \rightarrow Al_2O_3 \quad (8)$$

According to the information of SIGMA-ALDRICH Whatman® Anodisc Inorganic Filter Membrane, the price of anodic films are 526 USD for 200 nm pore size (47 mm sample size, 50 pieces) and 1,010 USD for 20 nm pore size (47 mm sample size, 50 pieces) (Whatman, 2015). Each anodic film are 10.5 and 20 USD. The high price of commercial films limits the structured anodic film to be widely used in the industry. In our previous results (Chen et al., 2015a; Chen et al., 2005; Chen et al., 2015b), we have successfully developed the processes to structured anodic aluminum oxide for a mass production. The obtained film sizes range from 0.1-200 cm^2, and the micro-structures are featured as 5-500 nm in pore size, 1-400 μm in film thickness, and 10^8-10^{12} pore/cm^2 in pore density. Furthermore, the producing cost of each AAO film can be controlled less than 0.5 USD/ piece.

In this paper, we have designed a novel electrochemical mold, which can overcome the exothermal effect during large-size aluminum sheet under a higher voltage anodization. Figure 7 shows the exploded views of electrochemical mold structure. The mold was made of acrylic and assembles with brass electrode. In Figure 7 (a), anode mold was a sandwich structure composed of the up-cover with a reaction window, the brass electrode, and the bottom-cover with a heat-transfer window. Figure 7 (b) presents a detail diagram of the exploded view of anode mold. Aluminum sample is set between the up-cover and electrode plate; the silicone rubber chips are used for the waterproof; and the electrode rod is contact to the electrode plate for applying anodic voltages to the Al sample. The porous-structured cathode plate is fixed between the acrylic plates and set on the anode surface, as shown in Figure 7 (c). A motor is the stirrer for removing the exothermal heat generated from Al surface. This electrochemical assembly is a convenient setup for any specific chemical bath.

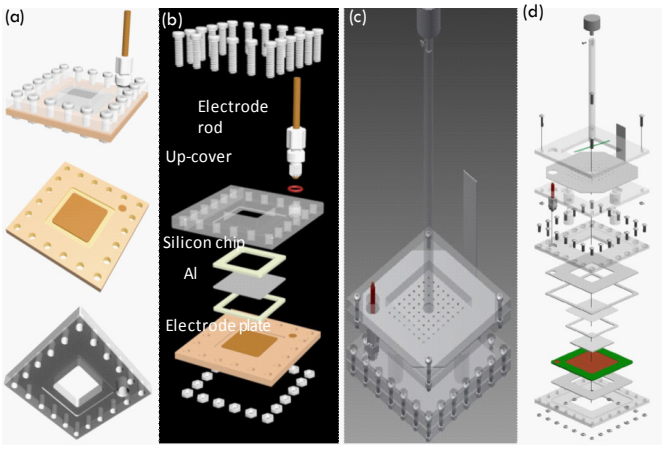

Figure 7. The assembled electrochemical mold made of acrylic; (a) anode mold, (b) exploded view of anode mold, (c) a cathode-anode mold with a motor as a stirrer , (d) exploded view.

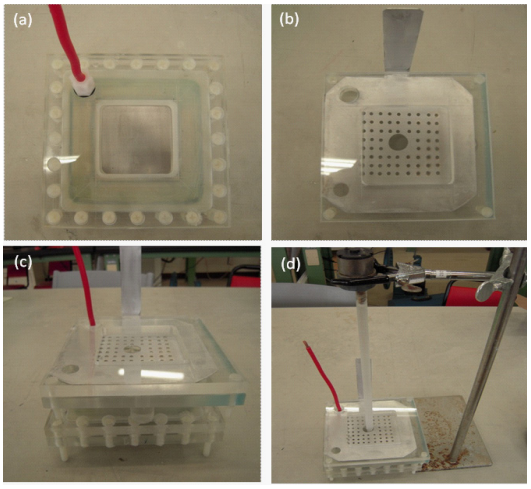

Figure 8. Images of the assembled electrochemical mold; (a) anode mold, (b) cathode mold, (c) a cathode-anode mold, (d) cathode-anode molds with a motor as a stirrer.

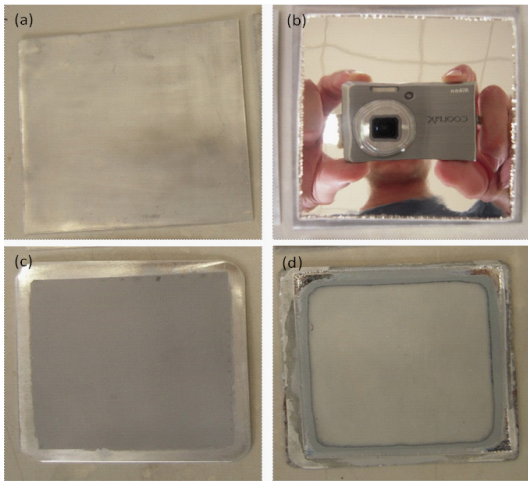

Figure 10. Images of 6 cm x 6 cm AAO film; (a) aluminum sheet after mechanical graining, (b) aluminum sheet after electrolytic polishing, (c) AAO film with Al substrate, (d) AAO film without Al substrate.

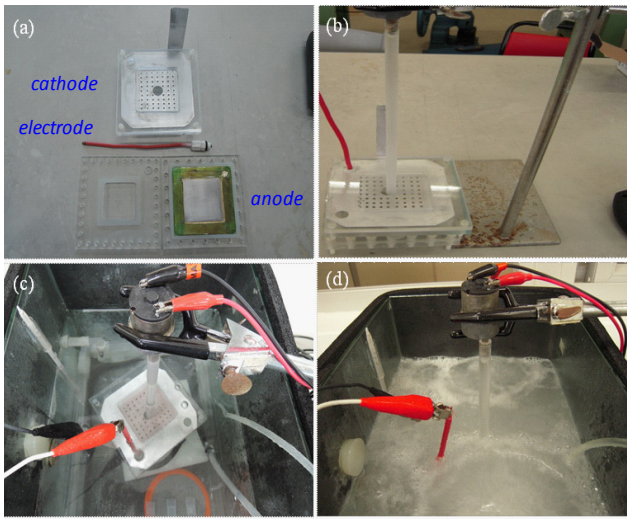

Figure 9. . The experimental setup for the AAO process; (a) electrochemical mold for AAO formation, (b) assembly electrochemical mold, (c) AAO formation in a anodization bath, (d) AAO formation in a anodization bath with a large among of bobble applied.

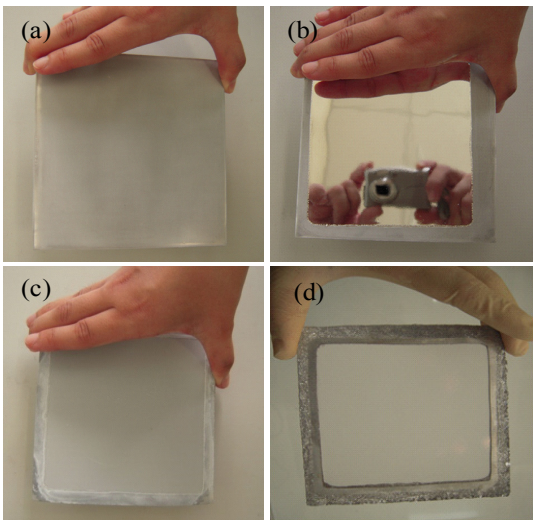

Figure 11. Images of 11 cm x 11 cm AAO film; (a) Al sheet after mechanical grained, (b) scratch-free surface after electrolytic polishing, (c) AAO film formation on the Al sheet, (d) An semitransparent AAO film.

Figure 7 (d) further shows the exploded view of electrochemical mold which is made of chip materials of brass plates, brass rod, acrylic plate, plastic screws and silicon chips.

Figure 8 shows the actual images of electrochemical mold. As shown in Figure 8(a) for the anode mold, the reaction window is adjustable to obtain various geometric areas. In the cathode mold, as shown in Figure 8 (b), the porous-structured metal cathode could dissipate the bobbles producing from the electrodes. The easy and convenient cathode-anode molds (Figure 8 (c)) can be easily carried and put into any reaction bath. In addition, cathode-anode molds with a stirrer could dissipate the bobbles and quickly remove the exothermal heat, as shown in Figure 8 (d).

Figure 9 shows the experimental setup for the AAO process. Figure 9 (a) displays the electrochemical mold, including a cathode plate with pores structure for the gas release, an anode up-cover with a fixed reaction area for anodization, and an bottom-cover with a fixed open area for heat transfer. In Figure 9 (b), electrochemical mold is assembled with a stirrer. Figure 9 (c) shows the mold set in the electrochemical bath for the AAO anodization process. Real working situation is further presented in Figure 9 (d). A large amount of bubbles is introduced to assist heat transfer while AAO anodized in the electrolyte bath.

Figure 10 shows the optical images of 6 cm x 6 cm anodic aluminum oxide (AAO) made with the assistance of designed electrochemical mold in the following steps. Step (a): most of rough scratches on aluminum sheet were removed after mechanical grinding. Step (b): a mirror-like aluminum surface was achieved after electrolytic polishing. Step (c): a uniformity AAO film was formed on Al surface through anodization process. Step (d): a translucent AAO film was obtained after removing Al substrate.

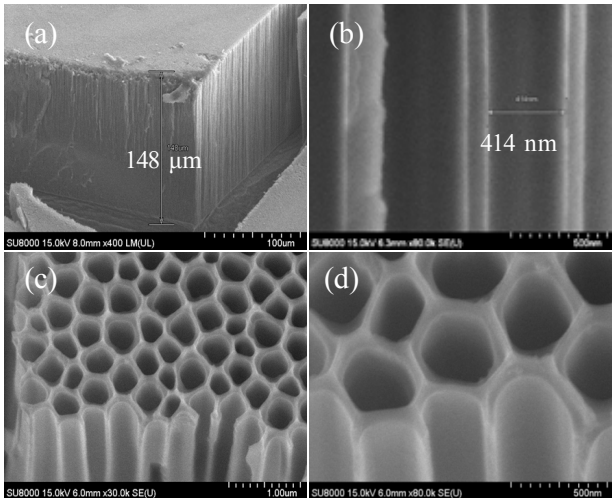

Figure 12. SEM images of AAO microstructure; (a)AAO with 148 µm thickness, (b) 414 nm pore size, (c) AAO with tubular structure, (d) AAO with hexagonal pore structure.

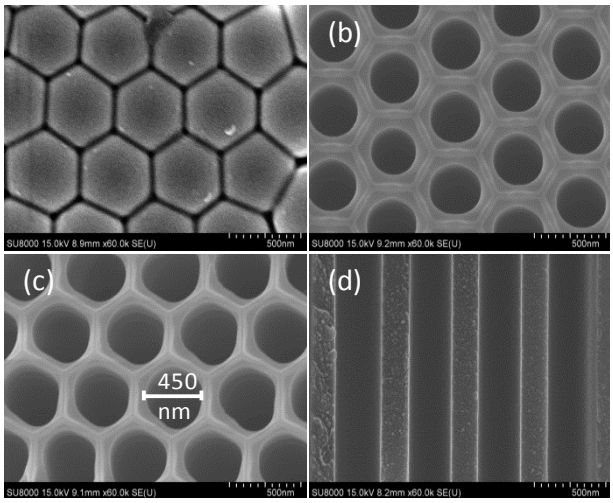

Figure 13. SEM images of AAO; (a) compact hexagonal barrier layer, (b) bottom pore under barrier layer, (c) top pore, (d) cross-section view of straight channel.

Furthermore, Figure 11 further shows the images of 11 cm x 11 cm AAO. In Figure 11 (a), high-purity (99.999%) Al sheet was mechanical grounded with #2400-grit sand paper. Figure 11 (b) shows mirror-like surface after electrolytic polishing in the solution of 15 vol.% $HClO_4$ + 70 vol.% C_2H_6O +15 vol.% $CH_3(CH_2)_3OCH_2CH_2OH$ at 42 V DC for 5 min. Figure 11 (c) shows AAO film formed on the Al surface through anodization process (1.5 vol.% H_3PO_4, 185V, 1 °C). A shown in Figure 11 (d), a translucent AAO film is obtained using conditions of 8 vol.% HCl + 10 wt.% $CuCl_2$ for 3 min.

In our precious results, the small-sized AAO films with pore sizes of 10-25 nm, 30-90 nm, and 180-500 nm, can be achieved respectively at 18 V for 10 vol.% H_2SO_4, 40 V for 3 wt.% $C_2H_2O_4$, and 195 V for 1 vol.% H_3PO_4. In this study, we furthermore improved the electrochemical mold and obtained a large-size AAO with the equivalent quality. Figures 12 (a-d)

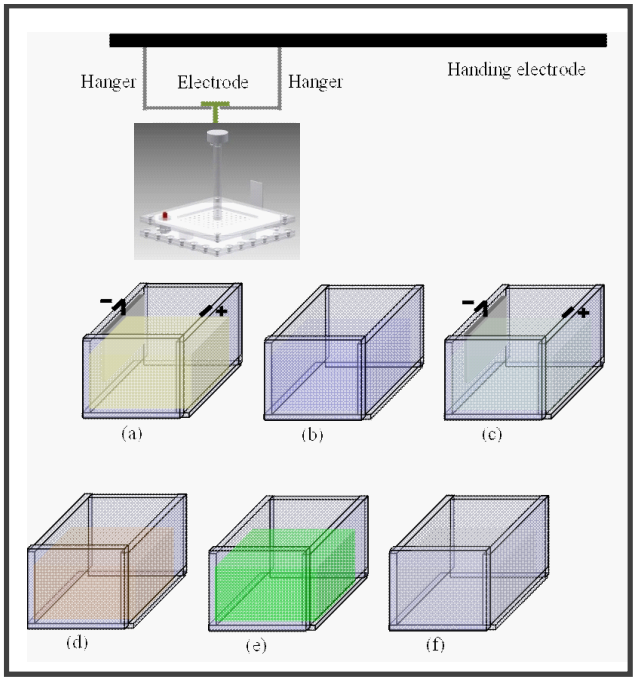

Figure 14. Schematic diagram of mass production of AAO film. The solutions in the tanks are (a) electro-polishing electrolyte, (b) water, (c) anodization electrolyte, (d) AAO removal solution, (e) aluminum removal solution, and (f) AAO pore widening solution.

show the SEM images of AAO microstructure anodized in 1.5 vol. % H_3PO_4 solution at 190 V. The thickness of obtained AAO is 148 µm after a 24 h anodization, and its dimension of characteristic tubular structure is about 414 nm.

Aluminum anodization with high applied voltage and low electrolyte is so-called hard anodizing, also known as hard-coating. The hard-coated aluminum has properties of high wearing and corrosion resistant for the industrial applications. The microstructure of AAO is an ordering hexagonal porous array due to the balance of tensile stresses under a suitable anodic condition. In our previous experiments, the arrangement of hexagonal pores raised with the anodic voltage increasing. For example, Figure 13 presents the SEM images of AAO anodized at 200 V. In Figure 13 (a), a barrier layer of ordering compact hexagonal structure was presented at AAO bottom. After barrier layer was removed the ordering bottom pore array was observed. Moreover, the average pore dimension is about 450 nm and of a straight-tubular arrangement. Comparing with Figure 12, the AAO formed at 200 V has more ordering arrangement pores than 190 V.

In order to reduce the cost of anodization process and to retain AAO's quality AAO, we designed a mass producing system for AAO film. Figure 14 shows the schematic diagram of an overhead conveyor system for the mass production of AAO film. The solutions of each tanks individually are (a) electropolishing electrolyte (HClO4 solution), (b) water, (c) anodization electrolyte (acid solution), (d) AAO removal solution (H_3PO_4 solution), (e) aluminum removal solution ($CuCl_2$ solution), and (f) AAO pore widening solution (H_3PO_4 solution). The operating order is sequentially from (a) to (f), but after each step the sample should

be returned to (b) bath. The anodization process must pass through solution reactions and water cleaning. For a quick and high-quantity AAO fabrication, we hence designed an overhead conveyor system with overhead hangers for the mass production of AAO film. The operation of each workstation will be non-synchronous since each production operation may have different processing time. Each overhead hanger will be controlled by its own motor and be operated independently based on different sensor inputs and processing times. Since there will be a limited number of stations (one station per tank), a single controller (RSLogix 5000) platform with Analog to Digital and Digital to Analog boards should be sufficient.

Conclusions

In this study, we proposed the advanced tools of electrochemical mold and designed the electrochemical system for anodization bath. The electrochemical mold and bath helped us successfully made a large-size submicron-structured AAO film. We also made high-quality and inexpensive thick AAO film that is a potential material for academic research and industrial applications. Some interesting findings in the present study are listed as follows.

(1) The high-quality anodic film can be controlled through electrochemical parameters including electrolyte temperature, electrolyte composition, electrolyte flow distribution, anodic voltage, current density on the working electrode, the distance between anode and cathode electrodes, the anode area relative to the cathode area, and the bobbles effect on the electrodes.
(2) Local heat should be quickly removed by cycling or agitating the electrolyte; otherwise, local pits, burrs, or cracks would present on AAO surface.
(3) Local heat can cause pits on AAO surface, resulting in failed AAO film during a higher voltage anodization.
(4) For a large-scale electrochemical reaction, the thermal effects are obvious. These severe thermal effects may destabilize the electrolyte temperature. A good electrochemical mold can assist to reduce the thermal effects and retain stable work piece temperature.
(5) The ordering compact hexagonal structure was formed on AAO surface because of the balance of tensile stresses under suitable anodic conditions. The order of hexagonal pores raised with anodic voltages increasing.

Acknowledgments

The authors gratefully appreciate the financial support of the Chung-Shan Institute of Science and Technology (CSIST) under the Contract No. CSIST-104-EC-17-A-22-0442

References

Barin I (1989) Thermochemical Data of Pure Substances. VCH verrlagsgesellschaftmbh, New York, USA, pp.17.

Chen CC, CG Kuo, and CG Chao (2015) Template Assisted Fabrication of Tin Nanospheres by Thermal Expansion and Rapid Solidification Process. Jpn. J. Appl. Phys. 44: 1524-1528.

Chen CC, CG Kuo, JH Chen, and CG Chao (2004) Nanoparticles of Pb-Bi Eutectic Nucleation and Growth on Alumina Template. Jpn. J. Appl. Phys. 43: 8354-8359.

Chen CC, CH Cheng, and CK Lin (2013) Template Assisted Fabrication of TiO_2/WO_3 Nanotubes. Ceram. Int. 39: 6631-6636.

Chen CC, CH Cheng, GY Tang, TN Lin, and CK Lin (2013) Template Assisted Fabrication of TiO_2 and $BaTiO_3$ Nanotubes. Appl. Mech. Mater. 271-272: 07-111.

Chen CC, CL Chen, and YS Lai (2013) The Enhancement of Platinum Surface Area by Alumina Template Assistance in Sn/Pt Core-Shell Nano/sub-micron Sphere Structure. Ceram. Int. 39: 4369-4375.

Chen CC, D Fang, and ZP Luo (2012) Fabrication and Characterization of Highly-Ordered Valve-Metal Oxide Nanotubes and Their Derivative Nanostructures. Rev in Nanosci and Nanotechnol 1: 229-256.

Chen CC, JH Chen, and CG Chao (2005) Post-treatment Method of Producing Ordered Array of Anodic Aluminum Oxide Using General Purity Commercial (99.7%) Aluminum. Jpn. J. Appl. Phys. 44: 1529-1533.

Chen CC, SF Chang, and ZP Luo (2013) Anodic-aluminum-oxide template assisted fabrication of cesium iodide (CsI) scintillator Nanowires. Mater. Lett. 112: 190-193.

Chen CC, SF Chang, MJ Kao, WD Jehng, and WS Hoa (2011) Fabrication of Thermo-conductivity Film Using Anodic Aluminum Oxide Template and Silver Nanowires. Adv. Mater. Res. 146-147: 22-25.

Chen CY, CW Hun, SF Chen, CC Chen, JS Lin, SS Johnson, N Noel, N Juliely, and ZP Luo (2015) Fabrication of Nanoscale Cesium Iodide (CsI) Scintillators for High-Energy Radiation Detection. Rev in Nanosci and Nanotechnol 4: 26-49.

Chen CY, SH Chen, CC Chen, and JS Lin (2015) Using Positive Pressure to produce a Sub-micron Single-Crystal Column of Cesium Iodide (CsI) for Scintillator Formation. Mater. Lett. 148: 138-141.

Chen PC, SJ Hsieh, CC Chen, and J Zou (2013) Fabrication and Characterization of Chemically Sensitive Needle Tips with Aluminum Oxide Nanopores for pH Indication. Ceram. Int. 39: 2597-2600.

Chen SH, CC Chen, and CG Chao (2009) Novel Morphology and Solidification Behavior of Eutectic Bismuth-Tin (Bi-Sn) Nanowires. J. Alloys Compd. 481: 270-273.

Lee W, K Schwirn1, M Steinhart1, E Pippel1, R Scholz1, and U Gösele1 (2008) Structural engineering of nanoporous anodic aluminium oxide by pulse anodization of aluminium. Nat. Nanotechnol. 3: 234-239.

Mardilovich P, AN Govyadinov, NI Mukhurov, AM Rzhevskii, and R Paterson (1995) New and modified anodic alumina membranes. Part I. Thermotreatment of anodic alumina membranes. J. Membr. Sci. 98: 131-142.

Spooner RC (1955) The Anodic Treatment of Aluminum in Sulfuric Acid Solutions. J. Electrochem. Soc. 102: 156-162.

Whatman® Anodisc Inorganic Membranes (2015) http://www.sigmaaldrich.com/labware/labware-products.html.

Ying JY, Z Zhang, L Zhang, and MS Dresselhaus (1998) Process for fabricating an array of nanowires. United States Patent: US6359288.